Inorganic Chemistry

Article

pubs.acs.org/IC

Tuning Reactivity of Diphenylpropynone Derivatives with Metal-Associated Amyloid-β Species via Structural Modifications

Yuzhong Liu,[†,‡,§] Akiko Kochi,[†,§] Amit S. Pithadia,[†] Sanghyun Lee,[‡,⊥] Younwoo Nam,[‡,▽] Michael W. Beck,[†] Xiaoming He,[‡,○] Dongkuk Lee,[▽] and Mi Hee Lim*[,†,‡]

[†]Department of Chemistry and [‡]Life Sciences Institute, University of Michigan, Ann Arbor, Michigan 48109, United States

[▽]Department of Fine Chemistry, Seoul National University of Science and Technology, Seoul 139-743, Korea

Supporting Information

ABSTRACT: A diphenylpropynone derivative, **DPP2**, has been recently demonstrated to target metal-associated amyloid-β (metal−Aβ) species implicated in Alzheimer's disease (AD). **DPP2** was shown to interact with metal−Aβ species and subsequently control Aβ aggregation (reactivity) in vitro; however, its cytotoxicity has limited further biological applications. In order to improve reactivity toward Aβ species and lower cytotoxicity, along with gaining an understanding of a structure-reactivity-cytotoxicity relationship, we designed, prepared, and characterized a series of small molecules (**C1**/**C2**, **P1**/**P2**, and **PA1**/**PA2**) as structurally modified **DPP2** analogues. A similar metal binding site to that of **DPP2** was contained in these compounds while their structures were varied to afford different interactions and reactivities with metal ions, Aβ species, and metal−Aβ species. Distinct reactivities of our chemical family toward in vitro Aβ aggregation in the absence and presence of metal ions were observed. Among our chemical series, the compound (**C2**) with a relatively rigid backbone and a dimethylamino group was observed to noticeably regulate both metal-free and metal-mediated Aβ aggregation to different extents. Using our compounds, cell viability was significantly improved, compared to that with **DPP2**. Lastly, modifications on the **DPP** framework maintained the structural properties for potential blood-brain barrier (BBB) permeability. Overall, our studies demonstrated that structural variations adjacent to the metal binding site of **DPP2** could govern different metal binding properties, interactions with Aβ and metal−Aβ species, reactivity toward metal-free and metal-induced Aβ aggregation, and cytotoxicity of the compounds, establishing a structure-reactivity-cytotoxicity relationship. This information could help gain insight into structural optimization for developing nontoxic chemical reagents toward targeting metal−Aβ species and modulating their reactivity in biological systems.

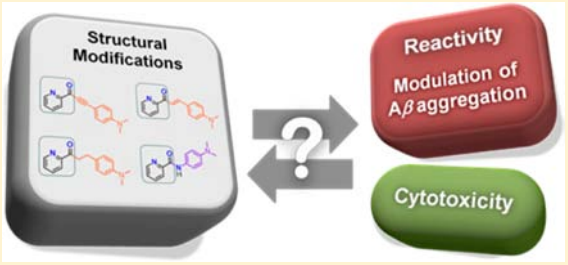

INTRODUCTION

Alzheimer's disease (AD) is a global economic and social issue, currently affecting 5.4 million Americans and an estimated 24 million people worldwide.[1] To date, there is no known cure for AD, and prevailing treatments only offer symptomatic relief for a short duration of time.[2−6] Recently, particular emphasis has been placed on therapeutics for misfolded amyloidogenic peptides, amyloid-β (Aβ) peptides, commonly found in AD brains.[2−7] The etiology of AD, however, remains elusive, because of the complexity emerging from the limited understanding of pathological features. The role of Aβ itself and its potential inter-relationships with other multiple factors, such as metal ion dyshomeostasis and oxidative stress, have been suggested.[2−6,8] Interactions between metal ions (e.g., Cu^{2+}, Zn^{2+}) and Aβ have been demonstrated to facilitate peptide aggregation and enhance oxidative stress via generation of reactive oxygen species.[2,3,6,8,9] The involvement of metal-associated Aβ (metal−Aβ) species in the onset and progression of AD, however, has been unclear and contentious, because of the limited availability of suitable chemical reagents to target metal−Aβ species and probe their link to neurotoxicity.

In order to elucidate potential associations of metal−Aβ species with AD pathogenesis, recent efforts have been made toward the development of chemical reagents to target metal−Aβ species, control the interactions between metal ions and Aβ species, and alter their reactivities (e.g., metal-triggered Aβ aggregation).[3,6,9,10] The structures of these reagents are rationally selected to achieve both metal chelation and Aβ interaction (bifunctionality).[11−16] Recently, a diphenylpropynone derivative (**DPP2**) was constructed through a rational structure-based design principle (incorporation approach), where a metal chelation site was directly installed into an Aβ interacting framework with minimal structural modifications (Figure 1).[16] **DPP2**, with a dimethylamino functionality, has demonstrated the ability to control both metal-free and metal-induced Aβ aggregation in vitro to different extents; however, because of its cytotoxicity, it could be only implemented for in vitro applications.[16] Further investigations on the structural modifications of **DPP2** would be valuable to improve its reactivity toward metal-free and metal-associated Aβ species

Received: April 6, 2013
Published: June 27, 2013

   dx.doi.org/10.1021/ic400851w | Inorg. Chem. 2013, 52, 8121−8130

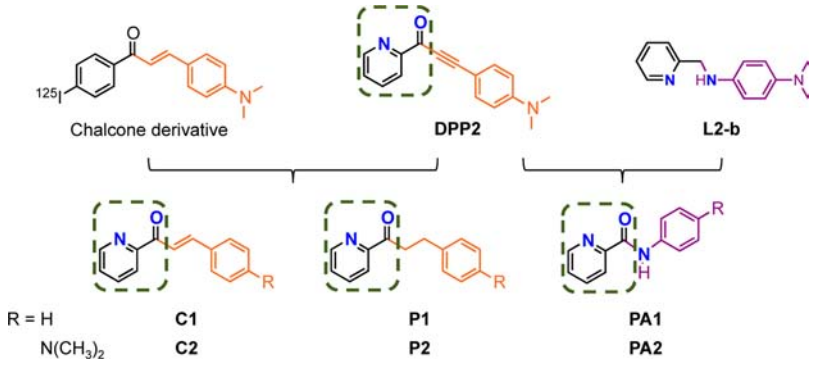

Figure 1. A class of **DPP** derivatives (**C1**/**C2**, **P1**/**P2**, and **PA1**/**PA2**). Chemical structures of chalcone derivative ([^{125}I]-(*E*)-3-(4-(dimethylamino)phenyl)-1-(4-iodophenyl)prop-2-en-1-one), **DPP2** (3-(4-(dimethylamino)phenyl)-1-(pyridin-2-yl)prop-2-yn-1-one), **L2-b** (N^1,N^1-dimethyl-N^4-(pyridin-2-ylmethyl)benzene-1,4-diamine), **C1** ((*E*)-3-phenyl-1-(pyridin-2-yl)prop-2-en-1-one), **C2** ((*E*)-3-(4-(dimethylamino)phenyl)-1-(pyridin-2-yl)prop-2-en-1-one), **P1** (3-phenyl-1-(pyridin-2-yl)propan-1-one), **P2** (3-(4-(dimethylamino)phenyl)-1-(pyridin-2-yl)propan-1-one), **PA1** (*N*-phenylpicolinamide), and **PA2** (*N*-(4-(dimethylamino)phenyl)picolinamide). Atoms for potential metal binding are highlighted in blue. The green box indicates metal chelation site from **DPP2**.

and cytotoxicity, as well as to establish a relationship between chemical structures, reactivity with Aβ and metal−Aβ species, and toxicity in cells. Thus, we present the design, preparation, characterization, and in vitro metal-free and metal-associated Aβ reactivity of a structurally modified **DPP2** series (**C1**/**C2**, **P1**/**P2**, and **PA1**/**PA2**; see Figure 1). The results and observations presented in this study illustrate that our structural variations on **DPP2** were shown to (i) tune metal binding and Aβ interaction properties of small molecules, thus altering their influence on both metal-free and metal-induced Aβ aggregation in vitro; (ii) reduce their cytotoxicity; and (iii) maintain their potential BBB permeability.

EXPERIMENTAL SECTION

Materials and Procedures. All reagents were purchased from commercial suppliers and used as received unless otherwise stated. The compounds (**C1**/**C2** and **PA1**/**PA2**) were synthesized following previously reported methods with modifications.[17−20] Aβ_{1-40} (DAEFRHDSGYEVHHQKLVFFAEDVGSNKGAIIGLMVGGVV) was purchased from Anaspec (Fremont, CA). Optical spectra for metal binding and solution speciation studies were recorded on an Agilent 8453 UV−visible (UV−vis) spectrophotometer. Nuclear magnetic resonance (NMR) spectra for the characterization of small molecules and Zn^{2+} binding studies were acquired on a Varian 400 MHz NMR spectrometer. Isothermal calorimetric titrations of Aβ_{1-40} with compounds were carried out with a MicroCal VP-ITC isothermal titration calorimeter (Northampton, MA). Transmission electron microscopy (TEM) images were recorded on a Philips CM-100 transmission electron microscope. A SpectraMax M5 microplate reader (Molecular Devices, Sunnyvale, CA) was used to measure the absorbance for MTT (3-(4,5-dimethylthiazol-2-yl)-2,5-diphenyltetrazolium bromide) and Parallel Artificial Membrane Permeability Assay adapted for Blood-Brain Barrier (PAMPA-BBB) assays.

Preparation of (*E*)-3-Phenyl-1-(pyridin-2-yl)prop-2-en-1-one (C1). A flask was charged with a mixture of 2-acetylpyridine (300 mg, 2.5 mmol) and benzaldehyde (285 mg, 2.7 mmol) in H_2O (15 mL). To the stirring mixture was added a 10% solution of NaOH (1.5 mL) dropwise. The mixture was stirred overnight at room temperature. The precipitates formed were filtered, washed with H_2O (3 × 10 mL), and dried over anhydrous $MgSO_4$. The product was concentrated in vacuo and purified by column chromatography (SiO_2, 100% CH_2Cl_2) to afford a yellow solid (450 mg, 2.2 mmol, 85%). ^{1}H NMR (400 MHz, $CDCl_3$)/δ (ppm): 7.42 (3H, m), 7.49 (1H, m), 7.73 (2H, m), 7.88 (1 H, dt, J = 7.6 and 1.6), 7.95 (1H, d, J = 16.0 Hz), 8.20 (1H, d, J = 8.0 Hz), 8.32 (1H, d, J = 16.0 Hz), 8.75 (1 H, m). ^{13}C NMR (100 MHz, $CDCl_3$)/δ (ppm): 189.4, 154.1, 148.8, 144.8, 137.0, 135.1, 130.5, 128.8, 126.9, 122.9, 120.8. HRMS: Calcd for $[M+H]^+$, 210.0841; found for $[M+H]^+$, 210.0913.

Preparation of (*E*)-3-(4-(Dimethylamino)phenyl)-1-(pyridin-2-yl)prop-2-en-1-one (C2). A flask was charged with a mixture of 2-acetylpyridine (242 mg, 2.0 mmol) and 4-dimethylaminobenzaldehyde (300 mg, 2.0 mmol) in EtOH (5 mL). To the stirring mixture was added a 20% solution of KOH (3 mL) dropwise. After stirring the mixture overnight at room temperature, H_2O (5 mL) was added to the flask before the red precipitates were filtered and washed with H_2O (5 mL) and cold EtOH (5 mL). The product was concentrated in vacuo and purified by recrystallization from CH_2Cl_2 and hexanes to afford dark orange crystals (352 mg, 1.4 mmol, 70%). ^{1}H NMR (400 MHz, $CDCl_3$)/δ (ppm): 3.05 (6H, s), 6.07 (2H, J = 9.2 Hz), 7.46 (1H, m), 7.64 (2 H, J = 9.2 Hz), 7.86 (1H, td, J = 7.6 and 2.0 Hz), 7.94 (1H, d, J = 16.0 Hz), 8.08 (1H, d, J = 16.0 Hz), 8.19 (1 H, d, J = 8.0 Hz), 8.73 (1 H, m). ^{13}C NMR (100 MHz, $CDCl_3$)/δ (ppm): 189.2, 155.0, 152.1, 148.7, 146.0, 136.9, 130.9, 126.4, 123.0, 122.8, 115.5, 111.7, 40.1. HRMS: Calcd for $[M+H]^+$, 253.1263; found for $[M+H]^+$, 253.1335.

Preparation of 3-Phenyl-1-(pyridin-2-yl)propan-1-one (P1). A flame-dried flask was charged with (*E*)-3-phenyl-1-(pyridin-2-yl)prop-2-en-1-one (300 mg, 0.71 mmol) and purged for 5 min prior to addition of dry CH_3OH (9 mL). To the stirring solution was added 10 wt % Pd/C (30 mg, 10 mol %) and Ph_2S (2.5 μL, 7.0 μmol). The reaction was allowed to stir under H_2 at room temperature for 24 h. The solution was then filtered through a 25-mm syringe filter, washed with CH_3OH (3 × 10 mL), and dried over anhydrous $MgSO_4$. The product was concentrated in vacuo and purified by column chromatography (SiO_2, 100% CH_2Cl_2) to afford an orange oil (108 mg, 0.51 mmol, 72%). ^{1}H NMR (400 MHz, $CDCl_3$)/δ (ppm): 3.07 (2H, t, J = 7.6 Hz), 3.57 (2H, t, J = 7.6 Hz), 7.18 (1H, q), 7.25−7.26 (4H, br), 7.45−7.42 (1H, m), 7.81 (1H, td, J = 9.2, 1.6 Hz), 8.02 (1H, dt, J = 8.0, 1.2 Hz), 8.64 (1H, d, J = 4.8 Hz). ^{13}C NMR (100 MHz, $CDCl_3$)/δ (ppm): 200.8, 153.4, 148.9, 141.7, 136.9, 128.4, 128.3, 127.1, 125.9, 121.5, 39.2, 29.8. HRMS: Calcd for $[M+H]^+$, 212.1070; found for $[M+H]^+$, 212.1070.

Preparation of 3-(4-(Dimethylamino)phenyl)-1-(pyridin-2-yl)propan-1-one (P2). A flame-dried flask was charged with (*E*)-3-(4-(dimethylamino)phenyl)-1-(pyridin-2-yl)prop-2-en-1-one (300 mg, 0.72 mmol) and purged for 5 min prior to addition of dry CH_3OH (9 mL). To the stirring solution was added 10 wt % Pd/C (30 mg, 10 mol %) and Ph_2S (2.5 μL, 7.0 μmol). The reaction was allowed to stir under H_2 at room temperature for 24 h. The solution was then filtered through a 25-mm syringe filter, washed with CH_3OH (3 × 10 mL), and dried over anhydrous $MgSO_4$. The product was concentrated in vacuo and purified by column chromatography (SiO_2, 1:1 ethyl acetate:hexanes) and washed several times with hexanes to afford the final product as a light green solid (93 mg, 0.37 mmol, 51%). ^{1}H NMR (400 MHz, CD_2Cl_2)/δ (ppm): 2.89 (6H, s), 2.93 (2H, t, J = 8.0 Hz),

dx.doi.org/10.1021/ic400851w | Inorg. Chem. 2013, 52, 8121−8130

3.48 (2H, t, J = 8.0 Hz), 6.67 (2H, d, J = 8.0 Hz), 7.11 (2H, d, J = 8.0 Hz), 7.47 (1H, ddd, J = 12.0, 4.0, 1.0 Hz), 7.83 (1H, td, J = 7.6, 1.6 Hz), 7.99 (1H, dt, J = 7.6, 0.8 Hz), 8.65 (1H, dd, J = 4.5, 1.2 Hz). ^{13}C NMR (100 MHz, CD_2Cl_2)/δ (ppm): 201.2, 153.5, 149.2, 148.9, 136.8, 129.8, 128.9, 127.1, 121.5, 112.9, 40.7, 39.6, 28.9. HRMS: Calcd for $[M+H]^+$, 255.1492; found for $[M+H]^+$, 255.1496.

Preparation of *N*-Phenylpicolinamide (PA1). A dried flask was charged with picolinic acid (123 mg, 1.0 mmol), followed by the addition of dry CH_2Cl_2 (10 mL). To the stirring mixture was added dicyclohexylcarbodiimide (DCC, 230 mg, 2.2 mmol), aniline (0.2 mL, 2.2 mmol), and 4-dimethylaminopyridine (DMAP, 50 mg, 0.45 mmol). After the mixture was stirred overnight at room temperature, H_2O (5 mL) was added to the flask before the white precipitates were filtered. The organic mixture was washed with H_2O (3 × 10 mL) and dried over anhydrous $MgSO_4$. The product was concentrated in vacuo and purified by column chromatography (SiO_2, 6:1 CH_2Cl_2:ethyl acetate) to afford a white solid (147 mg, 0.74 mmol, 74%). ^{1}H NMR (400 MHz, $CDCl_3$)/δ (ppm): 7.13 (1H, t, J = 7.4 Hz), 7.40 (2H, dd, J = 7.8, 8.1 Hz), 7.46 (1H, m), 7.78 (2H, d, J = 7.8 Hz), 7.89 (2H, dt, J = 1.8, 7.8 Hz), 8.29 (1H, d, J = 7.8 Hz), 8.60 (1H, d, J = 4.8 Hz). ^{13}C NMR (100 MHz, $CDCl_3$)/δ (ppm): 161.9, 149.8, 147.9, 137.7, 129.1, 126.4, 124.3, 122.4, 119.7. HRMS: Calcd for $[M+H]^+$, 199.0793; found for $[M+H]^+$, 199.0866.

Preparation of *N*-(4-(Dimethylamino)phenyl)picolinamide (PA2). A dried flask was charged with picolinic acid (123 mg, 1.0 mmol), followed by the addition of dry CH_2Cl_2 (10 mL). To the stirring mixture was added DCC (230 mg, 2.2 mmol), N^1,N^1-dimethylbenzene-1,4-diamine (149 mg, 2.2 mmol), and DMAP (50 mg, 0.45 mmol). After the mixture was stirred overnight at room temperature, H_2O (5 mL) was added to the flask before the white precipitates were filtered. The organic mixture was washed with water (3 × 10 mL) and dried over anhydrous $MgSO_4$. The product was concentrated in vacuo and purified by column chromatography (SiO_2, 5:1 CH_2Cl_2:ethyl acetate) to afford a yellow solid (190 mg, 0.79 mmol, 79%). ^{1}H NMR (400 MHz, $CDCl_3$)/δ (ppm): 2.93 (6H, s), 6.75 (2H, d, J = 9.0 Hz), 7.43 (1H, m), 7.63 (2H, d, J = 9.0 Hz), 7.86 (1H, dt, J = 1.7, 7.7 Hz), 8.27 (1H, d, J = 7.8 Hz), 8.58 (1H, d, J = 4.8 Hz), 9.82 (1H, s). ^{13}C NMR (100 MHz, DMSO)/δ (ppm): 162.0, 150.7, 148.7, 147.9, 138.5, 128.5, 127.0, 122.5, 121.8, 112.9, 40.9. HRMS: Calcd for $[M+H]^+$, 242.1205; found for $[M+H]^+$, 242.1292.

Amyloid-β (Aβ) Peptide Experiments. $A\beta_{1-40}$ peptide was dissolved with ammonium hydroxide (NH_4OH, 1% v/v, aq), aliquoted, lyophilized, and stored at −80 °C. A stock solution (ca. 200 μM) was prepared by redissolving Aβ with NH_4OH (1% w/v, aq, 10 μL) followed by dilution with doubly distilled (dd) H_2O, as reported previously.[12,13,21] Buffered solutions (20 μM HEPES (4-(2-hydroxyethyl)-1-piperazineethanesulfonic acid), pH 6.6 or 7.4, 150 μM NaCl) were used for both inhibition and disaggregation studies (pH 6.6 for Cu^{2+} samples;[22−24] pH 7.4 for metal-free and Zn^{2+} samples). For the inhibition experiment, Aβ (25 μM) was first treated with or without a metal chloride salt ($CuCl_2$ or $ZnCl_2$, 25 μM) for 2 min followed by addition of **C1**/**C2**, **P1**/**P2**, or **PA1**/**PA2** (50 μM, 1% v/v final DMSO concentration). The resulting samples were incubated at 37 °C for 4, 8, or 24 h with constant agitation. For the disaggregation experiment, Aβ in the absence or presence of a metal chloride salt ($CuCl_2$ or $ZnCl_2$) were initially incubated at 37 °C for 24 h with steady agitation. The compound was added afterward, followed by an additional 4, 8, or 24 h of incubation at 37 °C with constant agitation.

Gel Electrophoresis with Western Blotting. The Aβ peptide experiments described above were analyzed by gel electrophoresis, followed by Western blotting, using an anti-Aβ antibody (6E10).[12,13,21] Each sample (10 μL, [Aβ] = 25 μM) was separated using a 10−20% gradient Tris-tricine gel (Invitrogen, Grand Island, NY). The gel was transferred to a nitrocellulose membrane and blocked overnight with a bovine serum albumin (BSA) solution (3% w/v, Sigma, St. Louis, MO) in Tris-buffered saline (TBS, Fisher, Pittsburgh, PA) containing 0.1% Tween-20 (Sigma; TBS-T). The membrane was treated with the Aβ monoclonal antibody (6E10, Covance, Princeton, NJ; 1:2000; BSA, 2% w/v, in TBS-T) for 4 h at room temperature and then probed with a horseradish peroxidase-conjugated goat antimouse secondary antibody (1:5,000; Cayman Chemical, Ann Arbor, MI) in 2% BSA in TBS-T solution for 1 h at room temperature. The protein bands were visualized using Thermo Scientific Supersignal West Pico Chemiluminescent Substrate (Rockford, IL). Note that the gel analysis presented herein is qualitative due to properties of resulting Aβ species (e.g., sizes, conformations).

Transmission Electron Microscopy (TEM). Samples for TEM were prepared following a previously reported method.[12,13,21] Glow-discharged grids (Formar/Carbon 300-mesh, Electron Microscopy Sciences, Hatfield, PA) were treated with samples from either inhibition or disaggregation experiments (5 μL) for 2 min at room temperature. Excess sample was removed with filter paper and the grids were washed with ddH_2O five times. Each grid was stained with uranyl acetate (1% w/v ddH_2O, 5 μL) for 1 min. Uranyl acetate was blotted off and grids were dried for 15 min at room temperature. Images of samples were taken by a Philips Model CM-100 transmission electron microscopy (TEM) system (80 kV, 25 000× magnification).

Metal Binding Studies. The interactions of **C1**/**C2**, **P1**/**P2**, and **PA1**/**PA2** with Cu^{2+} and Zn^{2+} were investigated by UV−vis and ^{1}H NMR spectroscopy, respectively, based on previously reported procedures.[12,13,21] A solution of **C1**/**C2** (20 μM), **P1**/**P2** (50 μM), or **PA1**/**PA2** (50 μM) in EtOH was treated with 1−5 equiv of $CuCl_2$ with incubation of 2 min (for **C1**/**C2**) or 10 min (for **P1**/**P2** or **PA1**/**PA2**) at room temperature and was monitored by UV−vis. The interaction of **C1**/**C2**, **P1**/**P2**, or **PA1**/**PA2** with $ZnCl_2$ was observed by ^{1}H NMR spectroscopy upon the addition of 1−3 equiv of $ZnCl_2$ to a solution of **C1** (2 mM), **C2** (4 mM), **P1**/**P2** (4 mM), or **PA1**/**PA2** (8 mM) in acetonitrile-d_3 (CD_3CN). In addition, metal selectivity of **C1**/**C2**, **P1**/**P2**, and **PA1**/**PA2** was examined by measuring the optical changes upon addition of 1 equiv of $CuCl_2$ to a solution of ligand ([**C1**/**C2**] = 20 μM or [**P1**/**P2**] = [**PA1**/**PA2**] = 50 μM in EtOH) containing 1 or 25 equiv of another divalent metal chloride salt ($MgCl_2$, $CaCl_2$, $MnCl_2$, $FeCl_2$, $CoCl_2$, $NiCl_2$, or $ZnCl_2$). The Fe^{2+} samples were prepared by purging the solutions with N_2. Quantification of metal selectivity was calculated by comparing and normalizing the absorption values of metal−ligand complexes at 400 nm (for **C1**), 650 nm (for **C2**), 320 nm (for **P1**), 300 nm (for **P2**), 350 nm (for **PA1**), or 480 nm (for **PA2**) to the absorption at these wavelengths before and after the addition of $CuCl_2$ (A_M/A_{Cu}).

Solution Speciation Studies. The pK_a values for **C1**/**C2**, **P1**/**P2**, and **PA1**/**PA2** were determined by UV−vis variable-pH titrations following previously reported methods.[11,13,16] To obtain the pK_a values, a solution (10 mM NaOH, pH 12, 100 mM NaCl) of **C1**/**C2** (20 μM), **P1**/**P2** (50 μM), or **PA1**/**PA2** (50 μM) was titrated with small aliquots of HCl to obtain at least 30 spectra in the range of pH 2−10 (for **C1**/**C2** and **P1**/**P2**) or pH 1−12 (for **PA1**/**PA2**). In order to investigate the binding properties of ligands to Cu^{2+} at various pH values, a solution containing a compound ([**C2**] = 20 μM, [**P2**] = 50 μM, or [**PA2**] = 50 μM) and $CuCl_2$ in a ratio of 2:1 was incubated for 30 min, 2 h, and 30 min, respectively, and titrated with additions of HCl in a similar manner. At least 30 spectra were obtained over the range of pH 2−7 (for **C2** and **P2**) or pH 1−7.5 (for **PA2**). The acidity (pK_a) and stability (log β) constants were calculated by using the HypSpec program (Protonic Software, U.K.).[25] The speciation diagrams for **C1**/**C2**, **P1**/**P2**, **PA1**/**PA2**, Cu^{2+}−**C2**, Cu^{2+}−**P2**, and Cu^{2+}−**PA2** complexes were modeled by the HySS2009 program (Protonic Software).[26]

Isothermal Titration Calorimetry (ITC). Solutions of ligand (200 μM) and $A\beta_{1-40}$ (20 μM) in 20 μM HEPES buffer, pH 7.4, 150 μM NaCl (10% v/v DMSO) were prepared and degassed for 10 min prior to titration. The ligand solution (10 μL per injection) was injected over 1 s (25 times, with an interval of 200 s between each injection) into a solution of $A\beta_{1-40}$ (1.4 mL) using a motor-driven 250-μL syringe rotating at 310 rpm at 25 °C. As the control experiment, the ligand solution was injected into buffer solution without Aβ to measure the heat of dilution. Heat values of binding were measured by subtracting the heat of dilution value from the experimental results. Titration data were analyzed by using evaluation software (MicroCal Origin, Version 7.0). The binding curves were fitted with a one-site

dx.doi.org/10.1021/ic400851w | Inorg. Chem. 2013, 52, 8121−8130

binding or sequential model, affording the overall heat values of thermodynamic parameters.[27]

Docking Studies. Flexible ligand docking studies for **C1**/**C2** against the $A\beta_{1-40}$ monomer from the previously determined aqueous solution NMR structure (PDB 2LFM)[28] were conducted using AutoDock Vina.[29] Ten (10) conformations were selected from 20 conformations within the Protein Databank (PDB) file (1, 3, 5, 8, 10, 12, 13, 16, 17, and 20). The MMFF94 energy minimization in ChemBio3D Ultra 11.0 was used to optimize the ligand structures for docking studies. The structural files of **C1**/**C2** and the peptide were generated by AutoDock Tools and imported into PyRx,[30] which were used to run AutoDock Vina.[29] The search space dimensions were set to contain the entire peptide. The exhaustiveness for the docking runs was set at 1024. Docked poses of the ligands with Aβ were visualized using Pymol.

Cytotoxicity (MTT Assay). The human neuroblastoma SK-N-BE(2)-M17 cell line was purchased from the American Type Culture Collection (ATCC, Manassas, VA). The cell line was maintained in media containing 1:1 Minimum Essential Media (MEM, GIBCO, Grand Island, NY) and Ham's F12K Kaighn's Modification Media (F12K, GIBCO), 10% (v/v) fetal bovine serum (FBS, Sigma), 100 U/mL penicillin (GIBCO), and 100 mg/mL streptomycin (GIBCO). The cells were grown and maintained at 37 °C in a humidified atmosphere with 5% CO_2. M17 cells were seeded in a 96-well plate (15 000 cells in 100 μL per well), according to previously reported methods.[12,13,16,21] These cells were treated with various concentrations of **C1**/**C2**, **P1**/**P2**, or **PA1**/**PA2** (2.5−50 μM for **C1**/**C2**, 2.5−200 μM for **P1**/**P2** and **PA1**/**2**, final 1% v/v DMSO). After 24 h incubation at 37 °C, 25 μL MTT (5 mg/mL in phosphate buffered saline (PBS), pH 7.4, GIBCO) was added to each well and the plates were incubated for 4 h at 37 °C. Formazan produced by the cells was dissolved in a solution containing *N*,*N*-dimethylformamide (DMF, 50% v/v aq, pH 4.5) and sodium dodecyl sulfate (SDS, 20% w/v) overnight at room temperature. The absorbance (A_{600}) was subsequently measured on a microplate reader.

Parallel Artificial Membrane Permeability Assay Adapted for Blood-Brain Barrier (PAMPA-BBB). PAMPA-BBB experiments of compounds were carried out using the PAMPA Explorer kit (Pion, Inc. Billerica, MA) with modification to previously reported protocols.[13,16,31−33] Each stock solution was diluted with pH 7.4 Prisma HT buffer (Pion) to a final concentration of 25 μM (1% v/v DMSO) and was added to the wells of the donor plate (200 μL, number of replicates = 12). BBB-1 lipid formulation (5 μL, Pion) was used to coat the poly(vinylidene fluoride) (PVDF, 0.45 μM) filter membrane on the acceptor plate. The acceptor plate was placed on top of the donor plate, forming a sandwich, and brain sink buffer (BSB, 200 μL, Pion) was added to each well of the acceptor plate. The sandwich was incubated for 4 h at ambient temperature without stirring. UV−vis spectra of the solutions in the reference, acceptor, and donor plates were measured on a microplate reader. The PAMPA Explorer software, v. 3.5 (Pion), was used to calculate the value of $-\log P_e$ for each compound. CNS± designations were assigned by comparison to compounds that were identified in previous reports.[31−33]

RESULTS AND DISCUSSION

Design Consideration and Preparation of C1/C2, P1/P2, and PA1/PA2. A small molecule, **DPP2**, has been observed to target Aβ and metal−Aβ species and noticeably modulate metal-free and metal-induced Aβ aggregation in vitro to different extents; however, it presented cytotoxicity at low micromolar concentrations.[16] A series of compounds (**C1**/**C2**, **P1**/**P2**, and **PA1**/**PA2**; see Figure 1) were designed based on the structural modifications of **DPP2** in order to improve its reactivity with Aβ and metal−Aβ species, mitigate its cytotoxicity, and establish a structure-reactivity-cytotoxicity relationship. For the design of the compounds, the structural portion of **DPP2** for metal chelation, 2-pyridyl ketone,[16] was first retained in these frameworks (Figure 1). Metal chelation of **C1**/**C2** and **P1**/**P2** could occur through nitrogen and oxygen (N/O) donor atoms from 2-pyridyl ketone, while in **PA1**/**PA2**, N/O (2-pyridyl ketone) or N/N (pyridine and amide) donor atoms may be involved in metal binding.[34] Second, the triple bond with a carbonyl group (ynone) in **DPP2**, which may act as a Michael acceptor and cause cytotoxicity,[35−37] was modified (i.e., reduction or derivation of the triple bond; see Figure 1). This structural alteration could vary overall structural rigidity. **C1**/**C2** were produced via reduction of the triple bond to a double bond; the backbone of **C1**/**C2** was also found in the framework of an Aβ imaging agent, which is a chalcone derivative (Figure 1).[38] For **P1**/**P2**, the double bond was further reduced to a single bond. **PA1**/**PA2** were fashioned by combining the 2-pyridyl ketone moiety from **DPP2** and the aniline portion from **L2-b** via an amide moiety, instead of the carbon linker shown in **DPP2**, **C1**/**C2**, and **P1**/**P2**. Similar to **DPP2**, **L2-b** (Figure 1) was previously designed to serve as a potential chemical reagent to investigate metal−Aβ species in vitro and in living cells.[13] Lastly, a dimethylamino group, which has been suggested to be important for Aβ interaction,[13,16,39] was incorporated into the frameworks of **C2**, **P2**, and **PA2**. For preparation, **C1**/**C2** and **PA1**/**PA2** were synthesized based on previously reported methods with modifications (see Scheme S1 in the Supporting Information).[17−20] **P1**/**P2** were generated through the selective hydrogenation of **C1**/**C2** in the presence of 10 wt % Pd/C (see Scheme S1 in the Supporting Information).

Effects of C1/C2, P1/P2, and PA1/PA2 on Metal-Free and Metal-Induced Aβ Aggregation In Vitro. In order to understand the effect of structural variations on compound reactivity toward metal-free and metal-induced Aβ aggregation, inhibition (Figure 2) and disaggregation (Figure S1 in the Supporting Information) studies were conducted. Size distributions and morphologies of the resulting Aβ species from the two experiments were monitored by gel electrophoresis, followed by Western blot with an anti-Aβ antibody (6E10) and TEM, respectively.[12−16,21]

The influence of **C1**/**C2**, **P1**/**P2**, and **PA1**/**PA2** on formation of metal-free and metal-treated Aβ aggregates was first examined (inhibition studies; see Figure 2). Among these compounds, **C2** demonstrated the greatest reactivity with metal-free and metal-associated Aβ species to different extents, as confirmed by gel analysis. From metal-free Aβ aggregation with **C2** treatment, a wide molecular weight (MW) distribution of Aβ species was observed (Figure 2a, left, lane 3), which was also enhanced with prolonged incubation. Moreover, TEM images, obtained from the sample incubated with **C2** for 24 h (without metal ions), revealed thinner fibrils with diverse lengths, compared to those generated under compound-free conditions (Figure 2b). In the case of metal-triggered Aβ aggregation, **C2** presented differences in the control of Aβ aggregate formation in the reaction with Cu^{2+}−Aβ over that with Zn^{2+}−Aβ. Upon treating Cu^{2+}−Aβ species with **C2**, various-sized Aβ species were visualized by gel electrophoresis (Figure 2a, lane 6); while species (MW $\leq$ 25 kDa) were exhibited from the sample containing Aβ, Zn^{2+}, and **C2** (Figure 2a, lane 9). The modulation of Aβ aggregation by **C2** in the absence and presence of metal ions was also distinguished by TEM. A mixture of fibrils and amorphous aggregates (mainly, unstructured Aβ species) was detected in metal-treated conditions, whereas fibrils were mostly indicated from metal-free analogues.

dx.doi.org/10.1021/ic400851w | *Inorg. Chem.* 2013, 52, 8121−8130

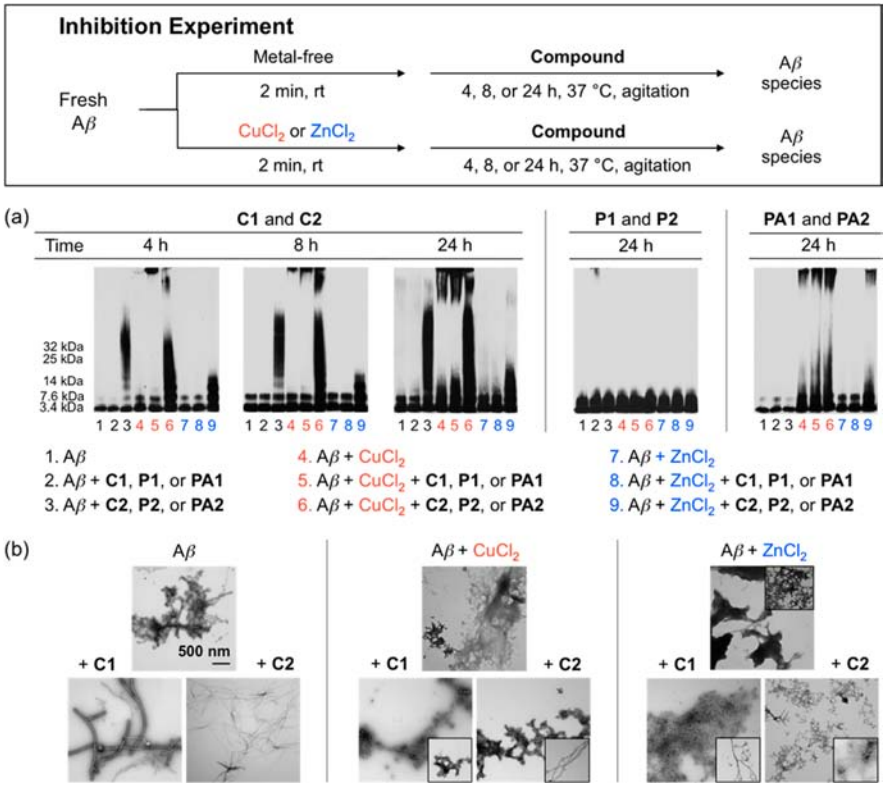

Figure 2. Inhibition experiment: modulation of Aβ aggregate formation in the absence and presence of metal ions (scheme, top) by **C1**/**C2**, **P1**/**P2**, or **PA1**/**PA2**: (a) analysis of the size distribution of the resulting Aβ species by gel electrophoresis with Western blot using an anti-Aβ antibody (6E10); and (b) visualization of the morphologies of the Aβ species from samples that were incubated with **C1** or **C2** for 24 h by TEM. Conditions: [Aβ] = 25 μM; [$CuCl_2$ or $ZnCl_2$] = 25 μM; [compound] = 50 μM (where "compound" = **C1**/**C2**, **P1**/**P2**, or **PA1**/**PA2**); pH 6.6 (for Cu^{2+} samples) or 7.4 (for metal-free and Zn^{2+} samples); various inhibition times; 37 °C; constant agitation.

As shown in Figure 2, alterations in structural scaffold differentiated reactivity toward Aβ aggregation (with and without metal ions). First, **C1**, which does not contain a dimethylamino group on the backbone compared to that of **C2** (Figure 1), did not significantly regulate the generation of Aβ aggregates (Figure 2a, left, lanes 2, 5, and 8). Second, as the carbon−carbon triple bond (C≡C) between two structural moieties (2-pyridyl ketone and dimethylaniline) in **DPP2**[16] was reduced to a double bond (C═C) in **C2** (Figure 1), the reactivity was changed toward Aβ aggregation in the absence and presence of metal ions. Under metal-free conditions, **C2** afforded Aβ species with a diverse range of MW starting from time points of 4−24 h, while **DPP2** exhibited less control on Aβ aggregation as time progressed.[16] Cu^{2+}-containing samples presented Aβ species with a various distribution of MW after 24 h with **C2** and **DPP2**.[16] Notably, this reactivity was more apparent with **C2** at early time periods. Aβ aggregates of MW < 25 kDa were indicated over time when treated with Zn^{2+} and **C2**. Aβ species (MW ≤ 25 kDa) were also observed in the case of **DPP2** at a short incubation time (e.g., 4 h), yet species showing different sizes were yielded after 24 h.[16] Third, upon substitution of the double bond in **C2** to a single bond in **P1**/**P2** (Figure 1), reactivity toward metal-free and metal-triggered Aβ aggregation disappeared (Figure 2a, middle). Lastly, for **PA1**/**PA2**, composed of 2-pyridyl ketone and an aniline portion via an amide linkage (Figure 1), some reactivity was detected toward Cu^{2+}-treated Aβ species after 24 h of incubation (Figure 2a, right, lanes 5 and 6). In addition, **PA2**, which has a dimethylamino functionality, showed slight modulation on Zn^{2+}-induced Aβ aggregation after 24 h (Figure 2a, right, lane 9). In contrast to their reactivity toward metal−Aβ, **PA1**/**PA2** did not display any significant influence on metal-free Aβ species even with longer incubation time. This general reactivity of **PA1**/**PA2** was distinct from that of **DPP2**[16] or **C2**.

Moreover, transformation of preformed metal-free and metal-induced Aβ aggregates by **C1**/**C2**, **P1**/**P2**, or **PA1**/**PA2** was also investigated (disaggregation studies; see Figure S1 in the Supporting Information). Upon incubation of these compounds, similar size distributions of resulting Aβ aggregates were confirmed by gel electrophoresis in comparison to those shown in the inhibition experiment (see Figure 2 and Figure S1 in the Supporting Information). In particular, **C2** was able to noticeably disassemble preformed metal-free and metal-mediated Aβ aggregates (Figure S1a in the Supporting Information). Aβ species generated from the disaggregation experiment employing **C2** displayed an array of MW and morphologies analogous to those in the inhibition studies (see Figure 2 and Figure S1 in the Supporting Information). The samples containing metal-treated Aβ species, followed by the addition of **DPP2**,[16] were visualized to have relatively more dispersion in MW than those with **C2**. In the metal-free condition, however, diverse-sized Aβ species were exhibited over longer incubation only in the presence of **C2**. As observed in inhibition studies, **C1** and **P1**/**P2** were not able to influence the disassembly of preformed Aβ aggregates in both metal-absent or metal-present cases; the modulation of these peptide aggregates was indicated with **PA1**/**PA2** only after 24 h. Thus, structural variations, such as the introduction of flexibility into the framework and/or incorporation of a dimethylamino

dx.doi.org/10.1021/ic400851w | Inorg. Chem. 2013, 52, 8121−8130

moiety, afforded altered reactivity with metal-free and metal-treated Aβ species in both inhibition and disaggregation studies. Both experiments suggest that **C2**, with a double bond replacing the triple bond in **DPP2**,[16] displayed the greatest control in regulating Aβ aggregate generation as well as disassembling preformed Aβ aggregates (both in the absence and presence of metal ions) to varying degrees in vitro. Furthermore, the backbones of **P** and **PA**, designed by further modification of the double bond in **C2** to a single bond and an amide bond, respectively, presented no or slight modulation on the formation or disaggregation of metal-free or metal-induced Aβ aggregates. Taken together, results and observations from both inhibition and disaggregation experiments imply that structural features, such as scaffold rigidity and substituents, may be essential for directing in vitro reactivity of small molecules toward metal-free and metal-associated Aβ aggregation.

Metal Binding Properties of C1/C2, P1/P2, and PA1/PA2. To investigate the effect of structural variation on metal binding properties of **C1**/**C2**, **P1**/**P2**, and **PA1**/**PA2** (containing a similar putative metal chelation site as **DPP2**, 2-pyridyl ketone[16]), the ability of **C1**/**C2**, **P1**/**P2**, or **PA1**/**PA2** to bind Cu^{2+} and Zn^{2+} was first examined by UV−vis and ^{1}H NMR spectroscopy, respectively (see Figure 3 and Figure S2 in the Supporting Information). As shown in Figure 3, changes in UV−vis spectra (i.e., new optical bands and/or change in absorbance intensity) were exhibited upon treatment of $CuCl_2$ (1−5 equiv) with **C1**/**C2**, **P1**/**P2**, or **PA1**/**PA2** in EtOH, indicating Cu^{2+} interaction of these compounds. Noticeable optical shifts from ca. 431 and 332 nm to 564 and 408 nm were detected after $CuCl_2$ treatment of **C2** and **PA2**, respectively. In addition to Cu^{2+} coordination, Zn^{2+} binding of **C1**/**C2**, **P1**/**P2**, and **PA1**/**PA2** were studied by ^{1}H NMR (see Figure S2 in the Supporting Information). NMR was employed for Zn^{2+} binding studies due to lack of significant optical changes of these ligands with $ZnCl_2$. The introduction of 1−3 equiv of Zn^{2+} to a CD_3CN solution of **C1**/**C2**, **P1**/**P2**, or **PA1**/**PA2** resulted in downfield chemical shifts of the pyridyl protons, demonstrating the involvement of the N donor atom from the pyridine ring (Figure 1) for Zn^{2+} binding. Moreover, the α and β protons of **C1**/**C2** and **P1**/**P2** displayed chemical shifts with Zn^{2+} treatment, which indicated that the O donor atom of the carbonyl group may also be associated in Zn^{2+} binding. In **PA1**/**PA2**, the amide proton shifted upfield and sharpened in the presence of Zn^{2+}, suggesting that the N donor atom of the amide moiety may be involved in metal coordination.[40,41] Overall, **C1**/**C2**, **P1**/**P2**, and **PA1**/**PA2**, generated via structural modification from **DPP2**, were able to bind to metal ions, such as Cu^{2+} and Zn^{2+}, possibly through the N and/or O donor atoms, similar to **DPP2**.[16]

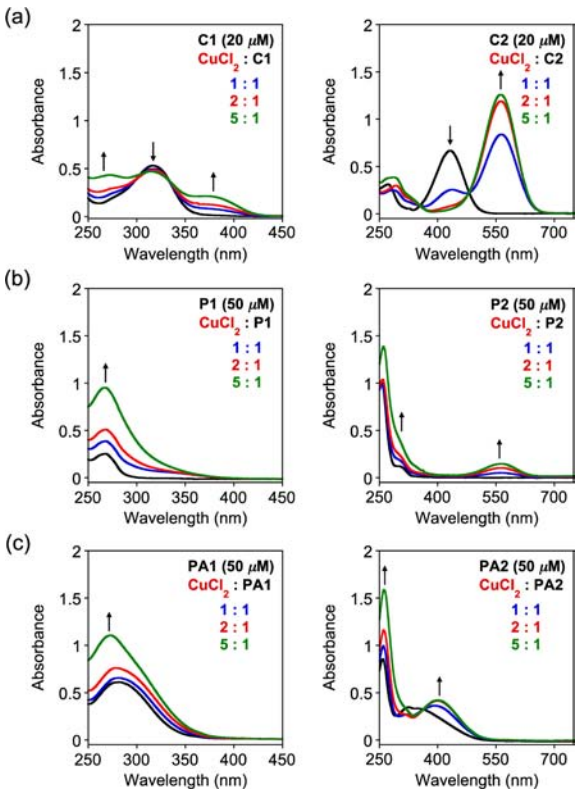

Figure 3. Cu^{2+} binding studies of **C1**/**C2**, **P1**/**P2**, and **PA1**/**PA2**. UV−vis spectra of (a) **C1** and **C2**, (b) **P1** and **P2**, and (c) **PA1** and **PA2** with $CuCl_2$ (1−5 equiv) in EtOH. Conditions: [**C1** or **C2**] = 20 μM; [**P1**/**P2** or **PA1**/**PA2**] = 50 μM; room temperature; incubation for 2 or 10 min.

To understand solution speciation of our chemical series in the absence and presence of Cu^{2+}, UV−vis variable-pH titration experiments were conducted.[11,13,16] Spectrophotometric titrations of compounds **C1**/**C2**, **P1**/**P2**, and **PA1**/**PA2** were first performed to estimate the acidity constant (pK_a) values (see Figure 4; **C1**, pK_a = 2.57(4); **C2**, pK_{a1} = 3.23(1), pK_{a2} = 4.00(1); **P1**, pK_a = 2.59(5); **P2**, pK_{a1} = 2.44(2), pK_{a2} = 5.40(4); **PA1**, pK_a = 1.69(9); **PA2**, pK_{a1} = 1.38(5), pK_{a2} = 4.91(8)). The diagrams depicted based on acidity constants indicated the presence of two forms of ligand (neutral and monoprotonated species; L and LH; L = **C1**, **P1**, and **PA1**; pK_a: protonation of the pyridyl N), as well as three forms of ligand (neutral, monoprotonated, and diprotonated species; L, LH, and LH_2; L = **C2**, **P2**, and **PA2**; pK_{a1}: protonation of the pyridyl N, pK_{a2}: protonation of the dimethylamino N) (Figure 4). The pK_{a2} values of **C2**, **P2**, and **PA2** are lower than that of **DPP2** (pK_{a2} = 7.01(6)),[16] which implies that neutral species would be present in a greater magnitude at a physiologically relevant pH (i.e., 7.4). Overall, all six compounds are expected to mainly exist in the neutral form at pH 7.4, suggesting their potential penetration through the blood-brain barrier (BBB; vide infra).[13,16,31−33]

Through solution speciation experiments of **C2**/**P2**/**PA2** in the presence of $CuCl_2$, their Cu^{2+} binding stochiometries, affinities, and the distribution of Cu^{2+}−ligand species were investigated (see Figure 5).[11,13,16] Based on the measured pK_a values of ligands above, the stability constants (log β) of Cu^{2+}−**C2**/**P2**/**PA2** complexes were first determined (see Figure 5; Cu + LH ⇌ Cu(LH) (log β_1); Cu + L ⇌ CuL (log β_2); Cu + 2L ⇌ CuL_2 (log β_3); for **C2**, log β_1 = 8.73(0), log β_2 = 5.62(8); for **P2**, log β_1 = 6.50(1), log β_2 = 3.76(9); for **PA2**, log β_1 =7.76(9), log β_2 = 4.17(7), log β_3 = 3.86(5)). Based on the log β values, greater stability of Cu^{2+}−ligand complexes was shown in the order of **C2**, **PA2**, and **P2**. Second, solution speciation diagrams were also modeled using these stability constants, indicating that (i) complexation occurred between Cu^{2+} and ligand in mainly 1:1 ratio (Cu:L; L = **C2**, **P2**, or **PA2**), (ii) free Cu^{2+}, CuL and Cu(LH) complexes were present in the solution containing Cu^{2+} and L (L = **C2** or **PA2**), and (iii) free Cu^{2+} and CuL complexes were shown in the sample of **P2**. At pH 7,[42] the complexes of CuL were present in solution at ca. 80%, 20%, and 40% for **C2**, **P2**, and **PA2**, respectively. From the diagrams,

dx.doi.org/10.1021/ic400851w | Inorg. Chem. 2013, 52, 8121−8130

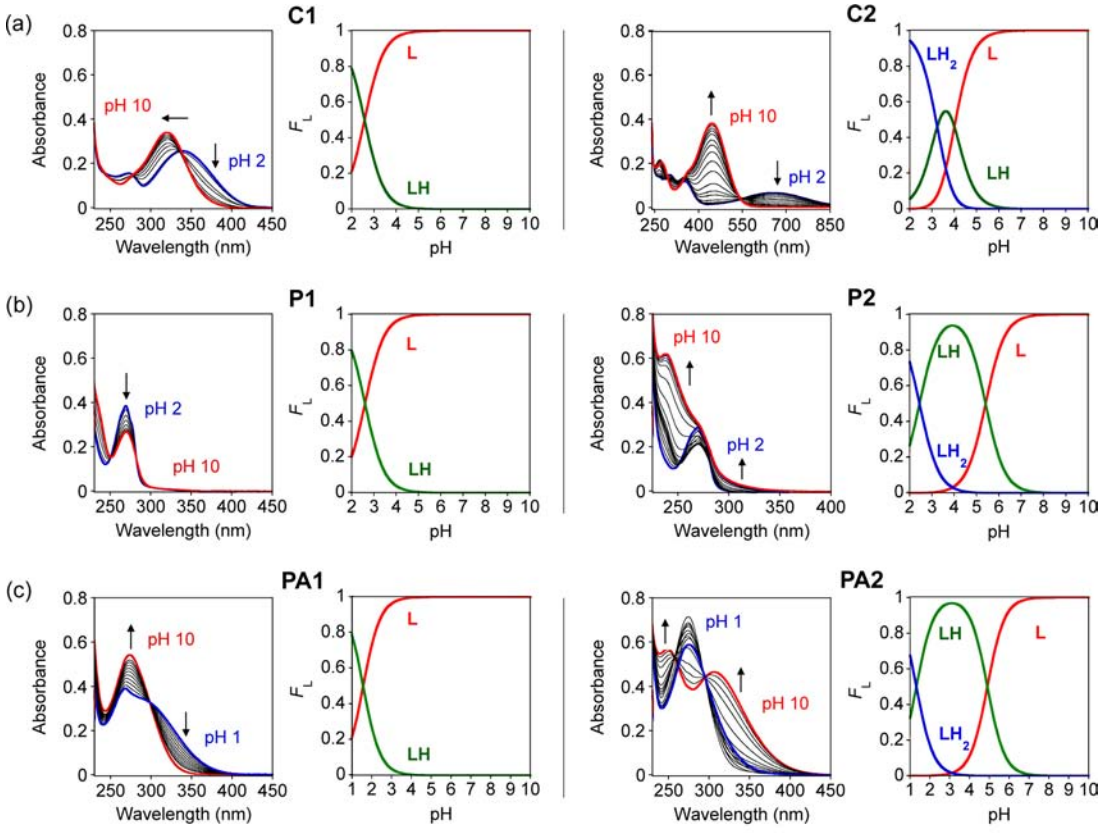

					pK_a[a]					
				L =	C1	C2	P1	P2	PA1	PA2
LH_2	⇌	LH	+ H	(pK_{a1})	–	3.23(1)	–	2.44(2)	–	1.38(5)
LH	⇌	L	+ H	(pK_{a2})	2.57(4)	4.00(1)	2.59(5)	5.40(4)	1.69(9)	4.91(8)

Figure 4. Solution speciation studies of **C1**/**C2**, **P1**/**P2**, and **PA1**/**PA2**. UV−vis variable-pH titration spectra (left) and solution speciation diagrams (right) of (a) **C1** and **C2** (pH 2−10), (b) **P1** and **P2** (pH 2−10), (c) **PA1** and **PA2** (pH 1−10) (F_L = fraction of species at the given pH). Acidity constants (pK_a) of L (L = **C1**/**2**, **P1**/**P2**, or **PA1**/**PA2**) are summarized in the table. Conditions: [L] = 20 μM (L = **C1** or **C2**) or 50 μM (L = **P1**, **P2**, **PA1**, or **PA2**); I = 0.10 M NaCl; room temperature. Charges are omitted for clarity. The superscript "a" in the table portion of the figure indicates that the error in the last digit is shown in the parentheses.

the values of pCu (pCu = $-\log[Cu_{unchelated}]$) of these compounds were also calculated to be 5.79, 4.70, and 4.81 at pH 6.6[22−24] for **C2**, **P2**, and **PA2**, respectively. Thus, the approximate dissociation constants ($K_d \approx [Cu_{unchelated}]$) for **C2**, **P2**, and **PA2** with Cu^{2+} were predicted to be in the micromolar range, making them slightly weaker metal chelators, compared to **DPP2** (pCu = 6.6, ca. low micromolar).[16] Different Cu^{2+} binding affinities of our ligands could result from the influence of electron density on the donor atoms for metal binding through structural variations (e.g., structural moieties between the 2-pyridyl ketone and aniline portions). Higher binding ability of **DPP2** and **C2** for Cu^{2+}, in comparison with those of **P2** and **PA2**, as well as Aβ interaction properties, may direct their ability to modulate Cu^{2+}-induced Aβ aggregation.

Furthermore, potential selectivity of **C2**, **P2**, and **PA2** for Cu^{2+} over other biologically relevant divalent metal ions (Mg^{2+}, Ca^{2+}, Mn^{2+}, Fe^{2+}, Co^{2+}, Ni^{2+}, and Zn^{2+}) was studied by competition reactions which were monitored by UV−vis. As depicted in Figure S3 in the Supporting Information, at an equimolar concentration of another metal ion and Cu^{2+}, the spectral changes after addition of Cu^{2+} indicated possible binding of compounds to Cu^{2+} in the presence of other divalent metal ions, similar to **DPP2**.[16] Moreover, these results may suggest a slightly higher selectivity for Cu^{2+} by **C2**, **P2**, and **PA2** in the solution containing $CoCl_2$ or $NiCl_2$, compared to **DPP2**.[16] At a supramolar ratio of another divalent metal ion to Cu^{2+} (25:1), **P2** seemed to be more selective for Cu^{2+} than **C2** and **PA2**.

Interaction of C1/C2 with Aβ Species Monitored by Isothermal Titration Calorimetry (ITC). In order to shed some light on possible interactions of **C1**/**C2**, **P2**, **PA2**, and **DPP2** with Aβ_{1-40}, isothermal titration calorimetry (ITC) experiments were performed, following previously reported methods.[27] Measured heat changes during the titration indicated potential interaction of our compounds with Aβ.[43] The titration data for **C1** and **C2** were fitted using a one-site binding model, whereas the data for **DPP2** were fitted with a sequential binding model (see Figure S4 in the Supporting Information). Based on the binding models, the best-fit values (binding stoichiometries (N), binding constants (K_A), enthalpy changes (ΔH), and Gibbs free energy (ΔG)) of these molecules were determined (see Table 1). The binding

dx.doi.org/10.1021/ic400851w | Inorg. Chem. 2013, 52, 8121−8130

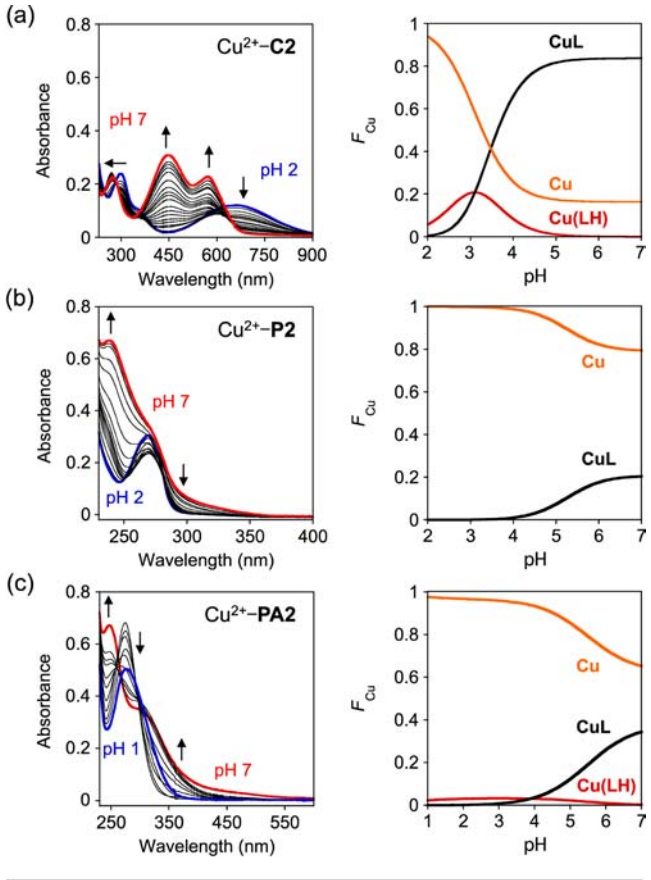

					logβ^a		
				L =	C2	P2	PA2
Cu	+	LH	⇌	Cu(LH)	8.73(0)	6.50(1)	7.76(9)
Cu	+	L	⇌	CuL	5.62(8)	3.76(9)	4.17(7)
Cu	+	2L	⇌	CuL_2	–	–	3.86(5)
pCu (= $-\log[Cu^{2+}]_{unchelated}$; pH 6.6)					5.79	4.70	4.81

Figure 5. Solution speciation studies of the Cu^{2+}–**C2**, Cu^{2+}–**P2**, and Cu^{2+}–**PA2** complexes. UV–vis variable-pH spectra (left) and solution speciation diagrams (right) of (a) Cu^{2+}–**C2** (pH 2–7), (b) Cu^{2+}–**P2** (pH 2–7), and (c) Cu^{2+}–**PA2** (pH 1–7) (F_{Cu} = fraction of free Cu and Cu-L complexes at the given pH). Conditions: $[Cu^{2+}]/[L]$ = 1:2, [L] = 20 μM (L = **C2**) or 50 μM (L = **P2** or **PA2**); incubation of ligand with Cu^{2+} for 30 min (L = **C2** and **PA2**) or 2 h (L = **P2**) prior to pH titration; room temperature. Stability constants (logβ) of Cu–L complexes are summarized in the table. Charges are omitted for clarity. The superscript "a" in the table portion of the figure indicates that the error in the last digit is shown in the parentheses.

affinities of all three ligands with Aβ were estimated to be in the same range (ca. 10^4–10^5 M^{-1}). The higher binding stoichiometry of **C2** to Aβ, compared to that of **C1**, however, implied that **C2** may be able to interact with Aβ to a greater extent (see Table 1). This may explain the better reactivity of **C2** toward Aβ species over **C1** observed from Aβ aggregation studies (vide supra; see Figure 2 and Figure S1 in the Supporting Information). **DPP2** also presented similar binding affinity toward Aβ as **C2**. Overall, **C2** and **DPP2** were shown to interact with Aβ in an energetically favorable manner (see Table 1).

Docking Studies for Possible Conformations of C1/C2 with Aβ. To visualize and further explore possible interactions between Aβ and **C1** or **C2**, docking studies were carried out using AutoDock Vina,[29] utilizing the previously determined NMR structure (PDB 2LFM)[28] of monomeric $A\beta_{1-40}$ (see Figure S5 in the Supporting Information). Aβ and **C1**/**C2** were observed to interact with each other through nonspecific and/or direct intermolecular interactions (e.g., hydrogen bonding, π–π stacking), with most conformations that exhibited **C1**/**C2** docking between the α-helix and the *N*-terminal random coil, similar to **DPP2**.[16] These interactions had calculated binding energies ranging from −5.8 to −4.9 kcal/mol and −5.9 to −4.8 kcal/mol for **C1** and **C2**, respectively (see Figure S5 in the Supporting Information). As shown in all conformations, **C1** and **C2** did not dock at the same sites on Aβ and were situated offset from each other when docked at similar sites (see Figure S5 in the Supporting Information). The observations from preliminary docking studies suggest that **C1** and **C2** could interact differently with Aβ, possibly related to the presence of a dimethylamino group in **C2**. This may further support the different reactivity toward Aβ aggregation of **C1** and **C2** in vitro (vide supra; see Figure 2 and Figure S1 in the Supporting Information).

Cytotoxicity of C1/C2, P1/P2, and PA1/PA2 in Living Cells. Cytotoxicity studies of **C1**/**C2**, **P1**/**P2**, and **PA1**/**PA2** have illustrated a potential relationship between molecular scaffolds and cytotoxicity. Human neuroblastoma SK-N-BE(2)-M17 cells were treated with various concentrations of compounds, and cell viability was measured using the MTT assay (see Figure 6).[13,16,21] Overall, through reduction of the conjugated triple bond to a double bond in **C1**/**C2**, cell viability (ca. 60% viability at 50 μM) was improved compared to that of **DPP2** (ca. 20% viability at 50 μM).[16] Furthermore, complete removal of the α,β-unsaturated moiety in **P1**/**P2** and **PA1**/**PA2** significantly mitigated the cytotoxicity of compounds (ca. 80% cell viability up to 200 μM concentration). Through structural modifications, we were able to improve the cytotoxicity of **DPP2**.[44]

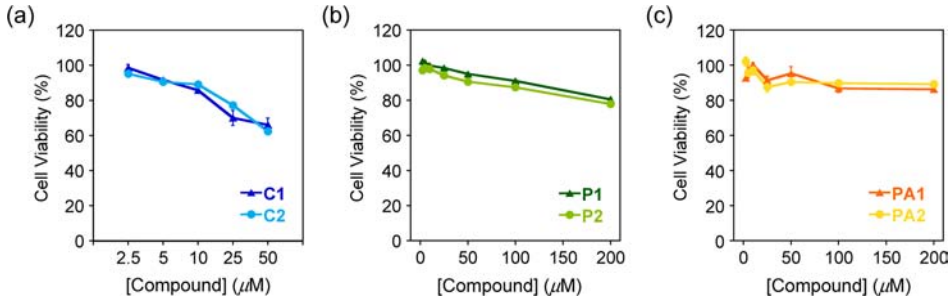

Figure 6. Cytotoxicity studies of **C1**/**C2**, **P1**/**P2**, and **PA1**/**PA2** in human neuroblastoma SK-N-BE(2)-M17 cells. Cells were treated with various concentrations of (a) **C1**/**C2** (2.5–50 μM), (b) **P1**/**P2** (2.5–200 μM), and (c) **PA1**/**PA2** (2.5–200 μM) for 24 h of incubation. Cell viability was determined by the MTT assay. Values of cell viability (%) were calculated relative to that of cells incubated only with 1% v/v DMSO. Error bars represent the standard deviation from at least three independent experiments.

dx.doi.org/10.1021/ic400851w | *Inorg. Chem.* 2013, 52, 8121–8130

Table 1. Thermodynamic Parameters of Interactions between C1/C2 or DPP2 with $A\beta_{1\text{-}40}$ at 25 °C

parameter	C1	C2	DPP2[a]
binding stoichiometry, N	0.88 ± 0.27	2.12 ± 0.06	–
binding constant, K_A (M^{-1})	2.38 ± 0.56 × 10^5	1.61 ± 0.26 × 10^5	4.06 ± 1.00 × 10^5 7.27 ± 1.26 × 10^4 3.97 ± 0.80 × 10^4
enthalpy change, ΔH (kJ/mol)	15.48 ± 9.16	10.93 ± 0.58	12.87 ± 0.21 × 10^5 33.70 ± 2.52 × 10^4 −15.18 ± 3.70 × 10^4
Gibbs free-energy change, ΔG (kJ/mol)	−0.69 ± 0.58	−29.72 ± 0.40	−32.01 ± 0.61 −27.75 ± 0.43 −26.25 ± 0.50

[a]Thermodynamic values for **DPP2** were calculated using a sequential binding mode.

Table 2. Values (MW, *c*logP, HBA, HBD, PSA, logBB, and $-\log P_e$) of C1/C2, P1/P2, and PA1/PA2

calculation	C1	C2	P1	P2	PA1	PA2	DPP2[a]	Lipinski's rules and others
molecular weight, MW	209	252	211	254	198	241	250	≤450
calculated logarithm of the octanol–water partition coefficient, *c*log*P*	2.92	3.09	2.98	3.14	1.26	1.43	2.63	≤5.0
hydrogen-bond acceptor atoms, HBA	2	3	2	3	3	4	3	≤10
hydrogen-bond donor atoms, HBD	0	0	0	0	1	1	0	≤5
polar surface area, PSA	30.0	33.2	30.0	33.2	42.0	45.2	33.2	≤90 Å^2
logBB[b]	0.131	0.108	0.139	0.116	−0.300	−0.323	0.0390	less than −1.0 (poorly distributed in the brain)
$-\log P_e$[c]	4.3 ± 0.1	4.2 ± 0.1	4.4 ± 0.1	4.3 ± 0.1	4.2 ± 0.1	4.2 ± 0.1	4.2 ± 0.1	$-\log P_e$ < 5.4 (CNS+) $-\log P_e$ > 5.7 (CNS−)
CNS± prediction[d]	CNS+	CNS+	CNS+	CNS+	CNS+	CNS+	CNS+	

[a]Values for **DPP2** have been previously reported.[16] [b]logBB = −0.0148 × PSA + 0.152 × *c*log*P* 0.130. [c]$-\log P_e$ values were determined using the Parallel Artificial Membrane Permeability Assay adapted for BBB (PAMPA-BBB). [d]Prediction of the ability of the compound to penetrate the central nervous system (CNS). Compounds categorized as CNS+ have the ability to permeate through the BBB and target the CNS. In the case of compounds assigned as CNS−, they have poor permeability through the BBB and, therefore, their bioavailability into the CNS is considered to be minimal.

Predicted Blood-Brain Barrier (BBB) Permeability of C1/C2, P1/P2, and PA1/PA2. To probe whether the scaffold modifications in the six compounds could retain structural parameters required for BBB permeability predicted with **DPP2**,[16] the values of Lipinski's rules and logBB were first calculated.[31,32,45,46] Based on the calculated values (see Table 2), all six compounds indicated drug-likeness and possible brain uptake. To confirm the potential BBB penetration prediction, an in vitro PAMPA-BBB assay was performed, following a previously reported method.[16,31−33] Based on the empirical classification of BBB-permeable molecules (e.g., verapamil),[16,31−33] the measured permeability values ($-\log P_e$), along with neutral speciation state at a physiologically relevant pH (vide supra; see Figure 4), suggest that **C1/C2**, **P1/P2**, and **PA1/PA2** could potentially permeate through the BBB and be available in the central nervous system (CNS+). Taken together, our structural alterations to **DPP2** did not seem to change the structural properties necessary for BBB permeability.

CONCLUSION

DPP2 derivatives, **C1/C2**, **P1/P2**, and **PA1/PA2**, were synthesized in order to improve reactivity of **DPP2** toward Aβ and metal−Aβ species and lower its cytotoxicity, as well as establish a structure-reactivity-cytotoxicity relationship. The ability of these structurally modified compounds to modulate in vitro metal-free and metal-induced Aβ aggregation was significantly distinct. Particularly, **C2**, having a double bond between two structural moieties (2-pyridyl ketone and dimethylaniline) and a dimethylamino group, displayed noticeable reactivity with both metal-free and metal-treated Aβ species. The difference in reactivity was associated with metal binding and Aβ interaction properties of our compounds, which were confirmed by solution speciation and ITC studies. In addition, an increase in cell viability was indicated with **C1/C2**, **P1/P2**, and **PA1/PA2**, relative to that with **DPP2**, possibly due to the alteration of the α,β-ynone moiety. Taken together, through structural modifications of **DPP2**, we demonstrate a relationship between structures, reactivity with Aβ and metal−Aβ, and cytotoxicity. The reactivity of our compounds with Aβ and metal−Aβ species, however, is shown to be limited in vitro;[44] therefore, further structural optimization for interacting with metal ions and/or Aβ species is desirable to accomplish their use in biological systems. Especially, the metal binding affinity of **C**, **P**, and **PA** could be improved through substitution of the carbonyl group in their backbones with a stronger metal binding group, such as an amino or hydroxyl moiety, as well as variation of denticity.

ASSOCIATED CONTENT

Supporting Information

Scheme S1 and Figures S1−S5 are available in the Supporting Information. This material is available free of charge via the Internet at http://pubs.acs.org.

dx.doi.org/10.1021/ic400851w | *Inorg. Chem.* 2013, 52, 8121−8130

AUTHOR INFORMATION

Corresponding Author

*E-mail address: mhlim@umich.edu.

Present Addresses

[⊥]Department of Molecular and Cellular Biology, University of Guelph, Guelph, Ontario N1G 2W1, Canada.

[○]Department of Chemistry, University of Calgary, Calgary, AB T2N 1N4, Canada.

Author Contributions

[§]These authors contributed equally.

Notes

The authors declare no competing financial interest.

ACKNOWLEDGMENTS

This study was supported by the Ruth K. Broad Biomedical Foundation, American Heart Association, and National Science Foundation (No. CHE-1253155) (to M.H.L.). D.L. thanks the Basic Science Program, through the National Research Foundation of Korea (NRF), funded by the Ministry of Education, Science and Technology (No. 2009-0087836) for the support. A.K. is grateful for the Research Excellence Fellowship from the Department of Chemistry at the University of Michigan. We thank Alaina DeToma and Whitney Smith for assistance of the PAMPA-BBB assay and the synthesis of **C1** and **C2**, respectively.

REFERENCES

(1) Alzheimer's Association. *Alzheimer's Dementia* **2012**, *8*, 131−168.

(2) Kepp, K. P. *Chem. Rev.* **2012**, *112*, 5193−5239.

(3) Scott, L. E.; Orvig, C. *Chem. Rev.* **2009**, *109*, 4885−4910.

(4) Jakob-Roetne, R.; Jacobsen, H. *Angew. Chem. Int. Ed.* **2009**, *48*, 3030−3059.

(5) Rauk, A. *Chem. Soc. Rev.* **2009**, *38*, 2698−2715.

(6) DeToma, A. S.; Salamekh, S.; Ramamoorthy, A.; Lim, M. H. *Chem. Soc. Rev.* **2012**, *41*, 608−621.

(7) Hardy, J. A.; Higgins, G. A. *Science* **1992**, *256*, 184−185.

(8) Savelieff, M. G.; Lee, S.; Liu, Y.; Lim, M. H. *ACS Chem. Biol.* **2013**, *8*, 856−865.

(9) Pithadia, A. S.; Lim, M. H. *Curr. Opin. Chem. Biol.* **2012**, *16*, 67−73.

(10) Rodríguez-Rodríguez, C.; Telpoukhovskaia, M.; Orvig, C. *Coord. Chem. Rev.* **2012**, *256*, 2308−2332.

(11) Rodríguez-Rodríguez, C.; Sánchez de Groot, N.; Rimola, A.; Álvarez-Larena, Á.; Lloveras, V.; Vidal-Gancedo, J.; Ventura, S.; Vendrell, J.; Sodupe, M.; González-Duarte, P. *J. Am. Chem. Soc.* **2009**, *131*, 1436−1451.

(12) Hindo, S. S.; Mancino, A. M.; Braymer, J. J.; Liu, Y.; Vivekanandan, S.; Ramamoorthy, A.; Lim, M. H. *J. Am. Chem. Soc.* **2009**, *131*, 16663−16665.

(13) Choi, J.-S.; Braymer, J. J.; Nanga, R. P. R.; Ramamoorthy, A.; Lim, M. H. *Proc. Natl. Acad. Sci. U.S.A.* **2010**, *107*, 21990−21995.

(14) Braymer, J. J.; Choi, J.-S.; DeToma, A. S.; Wang, C.; Nam, K.; Kampf, J. W.; Ramamoorthy, A.; Lim, M. H. *Inorg. Chem.* **2011**, *50*, 10724−10734.

(15) Sharma, A. K.; Pavlova, S. T.; Kim, J.; Finkelstein, D.; Hawco, N. J.; Rath, N. P.; Kim, J.; Mirica, L. M. *J. Am. Chem. Soc.* **2012**, *134*, 6625−6636.

(16) Pithadia, A. S.; Kochi, A.; Soper, M. T.; Beck, M. W.; Liu, Y.; Lee, S.; DeToma, A. S.; Ruotolo, B. T.; Lim, M. H. *Inorg. Chem.* **2012**, *51*, 12959−12967.

(17) Zakharychev, V. V.; Kuzenkov, A. V. *Chem. Heterocycl. Compd.* **2007**, *43*, 989−995.

(18) Singh, P. K.; Singh, V. K. *Org. Lett.* **2008**, *10*, 4121−4124.

(19) Carpino, L. A.; El-Faham, A. *J. Org. Chem.* **1995**, *60*, 3561−3564.

(20) Sasaki, K.; Crich, D. *Org. Lett.* **2011**, *13*, 2256−2259.

(21) Hyung, S.-J.; DeToma, A. S.; Brender, J. R.; Lee, S.; Vivekanandan, S.; Kochi, A.; Choi, J.-S.; Ramamoorthy, A.; Ruotolo, B. T.; Lim, M. H. *Proc. Natl. Acad. Sci. U.S.A.* **2013**, *110*, 3743−3748.

(22) Physiological acidosis has been observed in the AD brain (i.e., pH 6.6). To correlate diseased conditions, experiments were performed at a relevant pH. In addition, Aβ aggregation in the presence of Cu^{2+} was also suggested to be facilitated in a slightly acidic environment (see refs 23 and 24).

(23) Yates, C. M.; Butterworth, J.; Tennant, M. C.; Gordon, A. *J. Neurochem.* **1990**, *55*, 1624−1630.

(24) Atwood, C. S.; Moir, R. D.; Huang, X.; Scarpa, R. C.; Bacarra, N. M. E.; Romano, D. M.; Hartshorn, M. A.; Tanzi, R. E.; Bush, A. I. *J. Biol. Chem.* **1998**, *273*, 12817−12826.

(25) Gans, P.; Sabatini, A.; Vacca, A. *Ann. Chim.* **1999**, *89*, 45−49.

(26) Alderighi, L.; Gans, P.; Ienco, A.; Peters, D.; Sabatini, A.; Vacca, A. *Coord. Chem. Rev.* **1999**, *184*, 311−318.

(27) Wang, S.-H.; Liu, F.-F.; Dong, X.-Y.; Sun, Y. *J. Phys. Chem. B* **2010**, *114*, 11576−11583.

(28) Vivekanandan, S.; Brender, J. R.; Lee, S. Y.; Ramamoorthy, A. *Biochem. Biophys. Res. Commun.* **2011**, *411*, 312−316.

(29) Trott, O.; Olson, A. J. *J. Comput. Chem.* **2010**, *31*, 455−461.

(30) Wolf, L. K. *Chem. Eng. News* **2009**, *87*, 31.

(31) Di, L.; Kerns, E. H.; Fan, K.; McConnell, O. J.; Carter, G. T. *Eur. J. Med. Chem.* **2003**, *38*, 223−232.

(32) Avdeef, A.; Bendels, S.; Di, L.; Faller, B.; Kansy, M.; Sugano, K.; Yamauchi, Y. *J. Pharm. Sci.* **2007**, *96*, 2893−2909.

(33) *BBB Protocol and Test Compounds*; Pion, Inc.: Woburn, MA, 2009.

(34) Gomes, L.; Low, J. N.; Valente, M. A. D. C.; Freire, C.; Castro, B. *Acta Cryst.* **2007**, *C63*, m293−m296.

(35) Schultz, T. W.; Yarbrough, J. W. *SAR QSAR Environ. Res.* **2004**, *15*, 139−146.

(36) Koleva, Y. K.; Madden, J. C.; Cronin, M. T. D. *Chem. Res. Toxicol.* **2008**, *21*, 2300−2312.

(37) Sakagami, H.; Kawase, M.; Wakabayashi, H.; Kurihara, T. *Autophagy* **2007**, *3*, 493−495.

(38) Cui, M.; Ono, M.; Kimura, H.; Liu, B. L.; Saji, H. *Bioorg. Med. Chem. Lett.* **2011**, *21*, 980−982.

(39) Leuma Yona, R.; Mazères, S.; Faller, P.; Gras, E. *ChemMedChem* **2008**, *3*, 63−66.

(40) Xu, Z.; Baek, K.-H.; Kim, H. N.; Cui, J.; Qian, X.; Spring, D. R.; Shin, I.; Yoon, J. *J. Am. Chem. Soc.* **2010**, *132*, 601−610.

(41) Braymer, J. J.; Merrill, N. M.; Lim, M. H. *Inorg. Chim. Acta* **2012**, *380*, 261−268.

(42) Because of limited optical features at high pH (>8), solution speciation studies of Cu^{2+}−ligand complexes were conducted up to pH 7.

(43) The titration data for **P2** and **PA2** could not be fitted with any binding model.

(44) Mitigation of Aβ or metal−Aβ-induced toxicity by our compounds was further investigated; however, no noticeable influence on cell viability was observed (data not shown).

(45) Lipinski, C. A.; Lombardo, F.; Dominy, B. W.; Feeney, P. J. *Adv. Drug Delivery Rev.* **2001**, *46*, 3−26.

(46) Clark, D. E.; Pickett, S. D. *Drug Discovery Today* **2000**, *5*, 49−58.